Fuel 384 (2025) 133901

Contents lists available at ScienceDirect

Fuel

journal homepage: www.elsevier.com/locate/fuel

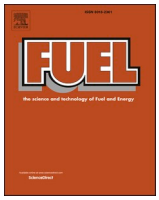

Full Length Article

Cost analysis of kerosene production from power-based syngas via the Fischer-Tropsch and methanol pathway

Stefan Bube *, Steffen Voß, Gunnar Quante, Martin Kaltschmitt

Hamburg University of Technology (TUHH), Institute of Environmental Technology and Energy Economics (IUE), Eißendorfer Straße 40, 21073 Hamburg, Germany

ARTICLE INFO

Keywords:
Kerosene production cost
Methanol-to-Jet (MtJ)
Fischer-Tropsch (FT) Synthesis
Power-to-Liquid (PtL)
Sustainable Aviation Fuel (SAF)
E-fuel

ABSTRACT

Current estimates for power-based kerosene production costs are up to ten times higher than conventional, fossil fuel-based kerosene prices. Therefore, successful market integration necessitates a thorough understanding of the cost structure and the key factors influencing kerosene production costs. This paper provides an extensive cost analysis of power-based kerosene production comparing two different plant concepts, one using the Fischer-Tropsch synthesis and hydrotreatment (FT pathway), the other applying direct methanol synthesis with downstream dehydration and oligomerization (MeOH pathway). Two cost allocation methods are applied to address uncertainties associated with unpredictable by-product revenues: allocating costs solely to the kerosene fraction, without considering by-product revenues, establishes the upper cost limit, while allocating costs at the total fuel fraction, defines the lower cost boundary. For these two cases, possible cost ranges are evaluated by varying technical and economic frame conditions. For the "total fuel allocation", the FT pathway yields lower kerosene production cost than the methanol pathway (FT: 3,630 €/t, MeOH: 4,240 €/t). But contrarily for the "kerosene allocation", the MeOH pathway shows lower cost (FT: 5,070 €/t, MeOH: 4,660 €/t). By-product revenue variation indicates benefits for the FT pathway if naphtha prices above 30 % of the kerosene production cost can be achieved. In all cases, costs are mainly affected by the supply of H_2 and CO_2; thus, feedstock conversion efficiency is the most important factor determining the production costs besides feedstock prices. While variations in the H_2 price (3 to 7 €/kg) significantly influence kerosene production costs for both pathways (ca. ± 25 %), CO_2 prices at the level of CO_2 supply costs from DAC (1,000 €/t) can lead to even higher cost increases of up to 75 % compared to CO_2 prices related to carbon capture costs from point sources (150 €/t). Thus, this analysis provides novel insights into the cost composition and the most important influencing parameters for the two most widely discussed production pathways for power-based kerosene production and enables comparison and assessment of production costs under different framework conditions.

1. Introduction

The global aviation sector strives to achieve net carbon dioxide neutrality by 2050 [1,2]. However, extensive decarbonization through direct electrification or using hydrogen (H_2), the most widely discussed options for land transport, seems technically and systemically unfeasible on a large scale for air transportation in the coming decades [3–5]. Furthermore, the globally available potential of biomass-based kerosene is limited due to the a priori restricted availability of sustainable biomass, enforced by significant competition from other sectors [6]. Consequently, fuels produced from renewable electricity and non-energetic feedstock (H_2O and CO_2), so-called power-based[1] or e-kerosene, are expected to play an essential role in reducing aviation's carbon dioxide emissions. The most common and widely developed pathways for producing power-based kerosene are the Fischer-Tropsch (FT) and the methanol (MeOH) pathway.

Abbreviations: ACC, Annual capital cost; DAC, Direct air capture; *FCI*, Fixed capital investment; *KPC*, Kerosene production cost; FT, Fischer-Tropsch; GHG, Greenhouse gas; HC, Hydrocracking; HHV, Higher heating value; K, Kerosene fraction; LTFT, Low-temperature Fischer-Tropsch; MeOH, Methanol; MtO, Methanol-to-Olefins; Oli, Oligomerization; PtL, Power-to-Liquid; PV, Parameter variation; RC, Reference case; RWGS, Reverse water–gas shift; SAF, Sustainable aviation fuel; TF, Total fuel product fraction; TRL, Technology readiness level; W, Wax; *WACC*, Weighted average cost of capital.

* Corresponding author.
E-mail address: stefan.bube@tuhh.de (S. Bube).

[1] In this paper, power is used as a substitute for electricity, as the production technology is a Power-to-X process, whereby power is used as an accepted term for electricity.

https://doi.org/10.1016/j.fuel.2024.133901
Received 13 September 2024; Received in revised form 12 November 2024; Accepted 25 November 2024
Available online 4 December 2024

Technically, the production of power-based kerosene is feasible, though it has not yet been commercially implemented [7,8]. The primary reason for the lack of commercially operated, large-scale production plants is economic uncertainty despite manageable technical risks. There is currently no established market for power-based kerosene, making long-term revenue projections difficult. Furthermore, studies indicate up to ten times higher production costs than fossil fuel-based kerosene and two- to threefold higher costs than biomass-based kerosene [9–15]. In a comprehensive analysis, Seymour et al. [16] analyzed the influence of geographical location on the production costs of power-to-liquid fuels and showed that in the medium term, even in very promising locations, the production costs are still significantly higher compared to conventional kerosene prices. Colelli et al. [17] analyzed a. o. production costs for power-based kerosene from FT synthesis, assessing indirect FT synthesis (incl. reverse water–gas shift reaction (RWGS) for CO_2 reduction) as technically and economically more beneficial compared to a direct CO_2-converting FT synthesis. The analysis from Raab and Dietrich [18] also takes supply chain aspects into account and finds that these only make a small contribution to the overall power-based kerosene costs. In a recently published detailed analysis of decentralized Fischer-Tropsch concepts, Meurer et al. [19] demonstrate that the advantages of decentralized production primarily stem from the reduction of indirect plant costs for modular units, although there are also disadvantages due to efficiency losses. Peacock et al. [20] investigated large-scale SAF production using FT synthesis, emphasizing the importance of a constant energy supply to achieve lower fuel production costs. While many available analyses provide a sound basis for general cost estimates of power-based fuel, differences within possible production pathways and influences of by-product revenues (and the respective cost allocations) are rarely considered. Moreover, most studies assume fixed technical and economic parameters, sometimes greatly influencing the cost outcomes and thus limiting the usability of the results. However, detailed consideration of process requirements and frame conditions is essential to compare different process pathways and identify the respective advantages and disadvantages. Recent technical analyses that compare process pathways at a high level of detail provide a suitable basis for economic considerations [7,21,22].

Against this background, this paper addresses these research gaps by providing a comprehensive cost analysis of kerosene production from power-based syngas, comparing two different plant concepts, one using the Fischer-Tropsch synthesis and hydrotreatment, the other applying direct methanol synthesis with downstream dehydration and oligomerization. This study provides valuable insights into both pathways' economic differences and advantages by evaluating the individual kerosene production cost based on identical system boundaries and framework conditions. Different cost allocations are applied to address uncertainties associated with unpredictable by-product revenues. An extensive variation of technical and economic parameters is carried out to derive sound cost ranges and to identify advantageous conditions for the respective process pathways.

The considered system boundaries with the primary process in- and outputs are depicted in Fig. 1. The analysis focuses on the synthesis and downstream processing, considering H_2 and CO_2 as feedstock. Kerosene is the targeted product, while naphtha and diesel are considered as by-products. The fuel fractions are categorized based on the chain length of the molecules. According to the system boundaries and in line with the general power-to-liquid (PtL) concept, electricity is considered as the primary energy source and, therefore, also for heat provision. Internally produced heat that exceeds the integrable quantity is considered for re-electrification via steam turbines so that only low-temperature heat (removed via cooling water) is produced in addition to the fuel products. The underlying concepts for the respective technical processes and simulation approaches are based on an in-depth technical analysis conducted by Bube et al. [7]. Therefore, only the main technical results are outlined in this study.

This paper is structured as follows. The methodology section details the production cost calculation methodology and the considered cost allocations. The subsequent section presents the main technical and economic assumptions, including the technical process concepts, feedstock prices, capital and operating expenditures, and variation parameters. The results of the analysis are then presented, including the process simulation results, detailed cost breakdowns, and parameter variation analysis. Finally, the results are summarized and discussed, and conclusions are derived.

2. Cost analysis methodology

Fig. 2 sketches the methodology used for the cost analysis based on prior process design and simulation. Cost calculation requires technical process data like operating conditions as well as mass and energy flows. The respective data is derived using steady-state flowsheet simulation, whereby the process design and simulation are mainly based on Bube et al. [7]. Modifications to the process concepts and modeling are defined in section 3.1 and the supplementary material. The cost analysis of the investigated process pathways is conducted for the presented process configurations and based on the described modeling approaches. Thus, the results are directly related to the specific process design, while alternative process concepts may lead to different results.

The cost analysis aims to derive and compare kerosene production costs from the analyzed process concepts under defined framework conditions. The individual cost components are analyzed at fixed technical and economic parameters (reference case, RC)(section 4.2). The influence of selected parameters on total costs is examined within a parameter variation (PV) (section 4.3).

The kerosene production cost represents the minimum required selling price to achieve economic feasibility in power-based fuel production (i.e., to cover all costs without assuming profit). According to Eq. (1), the annual total cost (*ATC*) consists of the annual capital costs (*ACC*), the fixed operational expenditures ($OPEX_f$) and the variable operational expenditures ($OPEX_v$). The latter represent the material and energy feedstock, while the fixed operational expenditures are costs considered to be independent of the product amount (e.g., labor, taxes, overheads, maintenance). The annual total cost can be transformed into kerosene production costs (*KPC*) according to Eq. (2), using different allocations with or without considering by-product revenues. Within multi-product generation plants, achievable prices for the by-products (here, power-based naphtha and diesel) can significantly impact the production cost of the targeted product (here, kerosene). Given the absence of established markets for power-based fuels and the reliance of their future value on the evolving regulatory framework, it is currently difficult to make reliable price assumptions. This analysis employs two different cost allocation approaches to address this challenge, providing an upper and lower bound for kerosene production costs and defining an expected cost range. The cost allocations impacting Eq. (2) are presented in Table 1.

- Within the kerosene allocation (KPC_K), only the kerosene fraction is considered a valuable product, with no by-product revenues accounted for, establishing the upper cost boundary.
- Conversely, the total fuel allocation (KPC_{TF}) assumes all fuel fractions (naphtha, kerosene, diesel) as valuable products, resulting in equal production costs for all fractions and defining the lower cost boundary.
- A variation of by-product revenues (*BPR*) is used to analyze trends in kerosene production costs (*KPC*) across both pathways and identify favorable *BPR* ranges for each pathway.

$$ATC = ACC + OPEX_f + OPEX_v \tag{1}$$

$$KPC = \frac{ATC - m_{BP} BPR}{m_P} \tag{2}$$

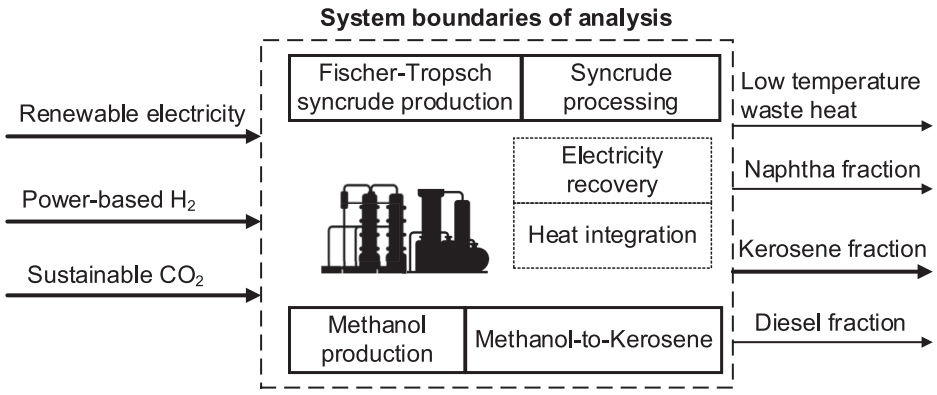

Fig. 1. System boundaries of considered power-based kerosene production pathways.

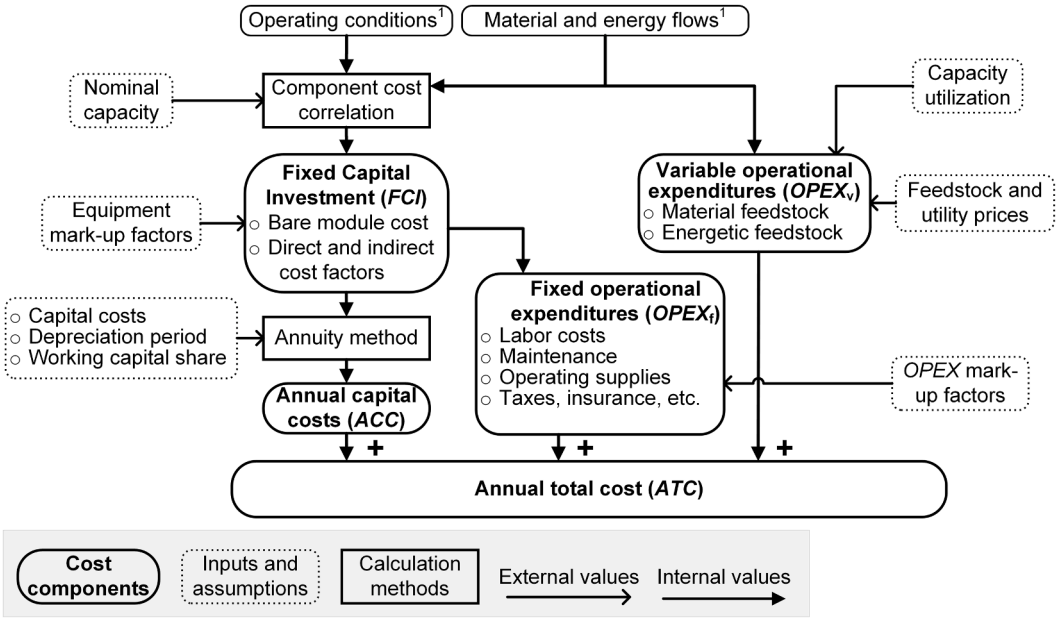

Fig. 2. Overall production cost calculation methodology. ([1] based on process design and simulation in accordance with [7])

Table 1
Allocation cases according to Eq. (2). (*BPR*: By-product revenue)

Key figure	Abbreviation	Product (P) | By-product (BP) [t]	*BPR* [€/t_{BP}]
Kerosene allocation	KPC_K	Kerosene | none	0
Total fuel allocation	KPC_{TF}	Naphtha, kerosene, diesel | none	0
Kerosene production cost	*KPC*	Kerosene | naphtha, diesel	varied

The annual production (m) is given by the nominal hourly output ($\dot{m}$) multiplied by the average capacity utilization (u) and the hours of one year (Eq. (3).

$$m = \dot{m}\, u\, 8{,}760\ \mathrm{h/a} \tag{3}$$

Annual capital cost. The annuity method (Eq. (4)) determines the annual capital cost. The capital required for the construction of the plant (fixed capital investment; *FCI*) is depreciated over the depreciation period (n[a]), taking into account the real weighted average cost of capital (*WACC*, i) and the working capital share (ω) [23].

$$ACC = FCI\,\frac{i\,(1+i)^n}{(1+i)^n - 1} + FCI\,\omega\,i \tag{4}$$

The fixed capital investment is derived using the module costing technique, a method for providing preliminary investment estimates for a.o. chemical plants [23]. This estimate is based on the major process equipment (k), which is roughly dimensioned using process design and simulation data. The size attribute A (e.g., area, volume, power, etc.) is used to calculate bare module costs (C_P^0) via equipment-specific component cost correlations (Eq. (5)) with empirical correlation parameters (K_x) given by Turton et al. [24]. The bare module costs are multiplied by equipment-specific mark-up factors, which depend on ($F_{BM,i}$) or are independent of ($F_{BM,i}^0$) operating conditions and construction material. The sum of all equipment costs multiplied by further mark-up factors for contingency and fee costs (γ) and auxiliary costs (β) results the fixed capital investment. This cost calculation method can be classified as a study estimate with an expected accuracy range of −30 to + 50 % [25].

$$\log_{10}(C_P^0) = K_1 + K_2 \log_{10}(A) + K_3 \left[\log_{10}(A)\right]^2 \tag{5}$$

$$FCI = \left(1+\gamma\right)\ \sum_{l=1}^{k} C^{0}_{\mathrm{P},l} F_{\mathrm{BM},l} + \beta \sum_{l=1}^{k} C^{0}_{\mathrm{P},l} F^{0}_{\mathrm{BM},l} \tag{6}$$

Fixed operational expenditures include labor costs, costs for maintenance, operating supplies, and other charges for royalties, distribution and selling, research and development, and so on. These costs are largely independent of production volumes. Empirical factors are used to estimate the individual cost items based on the fixed capital investment. Labor costs calculation is, among others, based on an estimate of the operating employee to allow for an uninterrupted operation throughout a calendar year.

Variable operational expenditures include costs for material and energetic inputs, i.e., H_2, CO_2, and electricity. The respective requirements are based on the process simulation and the technical evaluation of the plant concept specified in section 3. The specific prices to be applied are determined in accordance with the literature and vary within foreseeable ranges in the parameter variation. For feedstock for which there is currently no established market, the prices are defined based on the expected production costs.

Parameter variation. The variation of technical and economic parameters derives potential cost ranges and uncertainties resulting from different framework assumptions. For the variation of technical parameters, higher-level process parameters (e.g., conversion rates, selectivity) were chosen in line with the applied process modeling and, if applicable, defined in accordance with the state-of-the-art. The process concepts are simulated and analyzed for each varied parameter, whereby the same process conditions (e.g., inert gas concentrations, synthesis gas compositions, etc.) are ensured by defined design specifications. Since the varied higher-level process parameters can be achieved through multiple combinations of underlying operating conditions and design aspects (e.g., temperature, pressure, space velocity), which may interact in complex ways, such underlying parameters are considered constant during the parameter variation. This approach enables a more general evaluation at the system level with a manageable number of variables to be adjusted. The economic parameter variation is carried out for the technical reference case.

Further information on kerosene production cost calculation can be found in the supplementary material.

3. Data and assumptions

3.1. Technical concept assumptions

The following briefly describes the technical process concepts, the main assumptions, and the decisive technical parameters. Detailed information about the considered technologies, the respective modeling approaches, and the technical process analysis are available in [7]. Below, in particular, the differences made to [7] are highlighted.

The feedstocks H_2 (100 vol-%$_{H2}$, 50 bar, 35 °C [26,27]) and CO_2 (99.5 vol-%$_{CO2}$, 0.5 vol-%$_{N2}$, 1 bar, 35 °C [28]) are assumed to be available at the plant site. Process energy is constantly available grid electricity, covering the given electricity and heat demands. The fuel fractions naphtha (C_5 to C_8), kerosene (C_9 to C_{17}) [15,29], and diesel (C_{18} to C_{20}) can occur as material process outputs. The chain lengths included in the kerosene fraction are selected to ensure that ASTM conformity would be expected in real production processes. However, due to the lower component diversity in the simulation (no *iso*-alkanes, no cyclic components) compared to real products, ASTM conformity cannot be verified within the scope of the study. The properties of the kerosene fractions from the simulation, as well as the ASTM requirements, are presented and discussed in the supplementary material.

Three utility systems are considered in addition to the main processes. Vacuum generators are considered according to [30] (0.05 bar_a), enabling the rectification of heavy hydrocarbons at lower temperatures. Steam turbines serve to recover excess process heat as electricity, while furnaces are employed to generate high-temperature heat from light fuel gases. Heat integration (pinch analysis) is used to reduce external energy demands. Since excess heat is utilized in the steam turbines, only low-temperature waste heat (cooling water at 25 °C) leaves the system boundaries. A detailed description of the energy integration approach and the considered utilities is provided in the supplementary material.

3.1.1. Fischer-Tropsch pathway

Fig. 3 shows a block flow diagram of the FT pathway. The synthesis gas (syngas) production is carried out via a high-temperature (950 °C) reverse water–gas shift (RWGS) reaction, enabling parallel reforming of light hydrocarbons. The H_2:CO ratio in the produced syngas is set to 2.05 by adjusting the H_2 feed into the RWGS reactor. As the heat integration of the RWGS has a major influence on the overall efficiency of the process [31], feed gas preheating with the product gas is assumed. However, to counteract coking and metal dusting, the steam-to-carbon ratio in the reactor feed is set to 0.5.[2] Furthermore, preheating with product gas is limited to 200 K below the reactor temperature to enable rapid product gas cooling.[3] High-alloy nickel clad is chosen as a constructional countermeasure for the affected RWGS equipment [33]. The syngas is converted into synthetic crude oil (syncrude) using a low-temperature FT synthesis (LTFT) to produce a product mixture rich in long-chain hydrocarbons that is favorable in terms of overall process efficiency [7]. Heavy hydrocarbons (C_{18+}) are cracked via hydrocracking. Deviating to [7], hydrocracking is also applied to the diesel fraction. Thus, only naphtha and kerosene are produced.

Some technical parameters have a major influence on technical and, therefore, potentially also economic key figures. As described in the methodology, higher-level parameters are varied which can be influenced by different operating conditions and design aspects. In FT synthesis, a key parameter is the chain growth probability (α). It is the determining factor for the chain length distribution, i.e., mass fractions (W_n) of a component with the chain length n, in the FT product (Eq. (7)). This value typically ranges between 0.8 and 0.95 in the LTFT process and can be affected by factors such as temperature, syngas composition, pressure, residence time, and the catalyst used [35–38]. High chain growth probabilities can be achieved with cobalt catalysts under low temperatures (180 to 240 °C), elevated pressures, and sufficient residence time.

Another critical parameter in the FT pathway is the intensity of hydrocracking. In real processes, the intensity of hydrocracking is primarily adjusted by the reaction temperature and the catalyst used. Higher temperatures and more active catalysts increase the probability of cracking reactions. In the idealized cracking model used here, as described in [7,39], the intensity is approximated by the number of possible cracking reactions per molecule per reactor pass. Mild cracking is modeled assuming only one chain break (primary cracking), while severe cracking enables up to three cracking reactions per pass (tertiary cracking). The technical parameters assumed within the reference case and the parameter variation of the FT pathway are listed in Table 2.

$$W_n = n(1-\alpha)^2\alpha^{n-1} \tag{7}$$

3.1.2. Methanol pathway

No design changes are made in the methanol pathway compared to [7]. Fig. 4 shows the simplified block flow diagram of the respective

[2] In steam methane reforming the steam-to-carbon ration is usually around 1.5, but water is consumed during the reaction in a similar proportion as CO is formed [32]. Since the RWGS reaction is a steam generating reaction, the ratio in the RWGS was adjusted accordingly to 0.5.

[3] Metal dusting occurs with CO rich gases mainly between 400 and 800 °C [32,33] The risk of metal dusting can be reduced via fast cooling (commonly performed in a high pressure steam quench [34]) to restrict carbon formation kinetically.

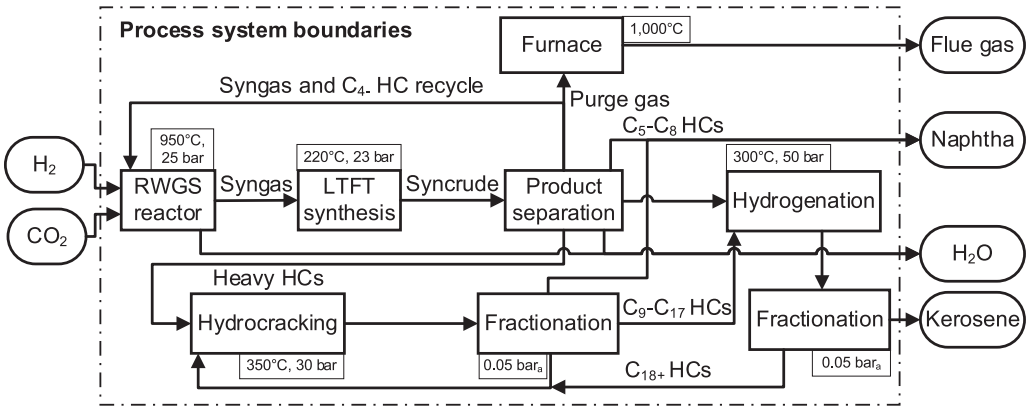

Fig. 3. Fischer-Tropsch pathway block flow diagram. (Only main processes shown; LTFT: Low-temperature Fischer-Tropsch, HC: Hydrocarbon, RWGS: Reverse water–gas shift)

Table 2
Technical parameters for the reference case and parameter variation of the Fischer-Tropsch pathway. (RC: Reference case, PV: Parameter variation)

Process	Parameter	Value
FT synthesis	Chain growth probability (α_{FT})	RC: 0.89 PV: 0.84–0.94
Hydrocracking	Ideal cracking; chain length depending conversion	RC: Secondary cracking PV: Primary to tertiary cracking

process concept. The methanol produced in the direct (CO_2-converting) methanol synthesis is converted via dehydration (methanol-to-olefin, MtO) into light olefins (mainly ethene and propene). The product mixture is cleaned (water and caustic wash, drying via molecular sieves) and fed into the oligomerization. Different catalysts in multi-stage or multi-bed reactors are used to ensure high conversions of all olefins. Nickel-based catalysts allow for nearly complete conversion of ethene [40]. Subsequent oligomerization using acid catalysts (e.g., in mesoporous and microporous materials, zeolites, or resins) enables the production of a high proportion of highly branched C_{10+} olefins [40,41]. The oligomerization product is fractionated into lighter hydrocarbons (C_{8-}), mainly recycled to increase the overall kerosene fraction, and a heavier hydrocarbon fraction (C_{9+}), which is hydrogenated and further fractionated. Since no waxes are formed in this process, no hydrocracker is considered. Therefore, diesel is also produced in addition to kerosene and naphtha.

Within the MeOH pathway, the technical analysis (see [7]) indicates the strong influence of MtO olefin selectivity (S_O) and oligomerization chain growth probability. The achievable olefin selectivity, defined as the proportion of carbon in methanol that is converted into olefins, is approximately 80 to 90 % in industrial processes [42,43]. Ongoing research, particularly in catalyst development, is focused on achieving even higher selectivities. As in FT synthesis, oligomerization can also be characterized by chain growth probability. However, the monomers can consist of various olefins from the MtO reactor or the oligomerization recycle stream. Depending on the reactant composition and the target product (i.e., chain length and component type), oligomerization can occur via various technologies, primarily distinguished by the catalysts used. The chain length distribution can be influenced by the catalyst and factors such as reactor temperature, pressure, residence time, and feed composition [40,41]. High temperatures and short residence times tend to reduce the chain growth probability. The generic model used here for oligomerization is described in detail in the supplementary material. Due to the variety of oligomerization processes and the large number of influencing parameters, significant differences in product distributions can potentially occur in real oligomerization processes. Therefore, the chain growth probability in this study varies across a wide range within the parameter variation. Table 3 lists the parameters considered within the reference case and the parameter variation.

Table 3
Technical parameters for the reference case and parameter variation of the methanol pathway. (RC: Reference case, PV: Parameter variation).

Process	Parameter	Value
Dehydration (MtO)	Olefin-Selectivity (S_O)	RC: 0.90 PV: 0.85–0.95
Oligomerization	Chain growth probability (α_{Oli})[a]	RC: 0.3 PV: 0.2–0.4

[a] Advanced oligomerization modeling compared to [7] (see supplementary material).

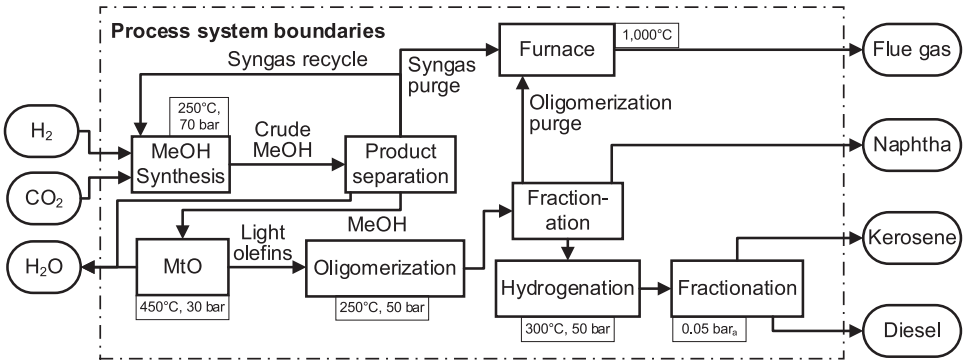

Fig. 4. Methanol pathway block flow diagram. (Only main processes shown; MeOH: Methanol, MtO: Methanol-to-Olefins)

3.2. Economic data and assumptions

Besides the technical data and assumptions primarily used for process modeling and simulation, further parameters predominantly affect economic figures and do not change technical results. The main economic parameters here are described and listed below (Table 4).

The plant investments are calculated for a market-mature process (n^{th}-of-a-kind plant) built on a green field. The installed production capacity for both pathways at 8,760 h/a at nominal load is around 100 kt_{TF}/a, corresponding to the largest PtL projects currently targeted [8]. However, as most of the currently planned projects have significantly lower capacities, while conventional fuel productions (e.g., via gas-to-liquid (GtL)) have significantly higher installed capacities, the production capacity is varied within the parameter variation. The cost functions and factors used to calculate the costs for the construction and commissioning of the plant (fixed capital investment) are listed in detail in the supplementary material.

The capacity utilization determines the annual production quantity at a given plant capacity, thus impacting the production costs. It depends on the customers' demand, the feedstock availability, and the plant reliability. The cost of feedstock availability, especially for H_2 from renewable energy and CO_2 of sustainable (non-fossil) origin, depends strongly on the plant location (availability and timing of renewable energy) and the infrastructure (existing H_2 and CO_2 grid). Since the constant supply of H_2 requires large, sometimes seasonal, storage facilities and overcapacities of the corresponding production facilities, which increases the cost of H_2 [44], it is assumed that capacity utilization of the conversion plants will be lower than for conventional plants which operate at an average of 75 to 85 % [45]. However, since this can vary greatly depending on the locally given frame conditions, the parameter variation also considers capacity utilization.

The fixed capital investment (*FCI*) depreciation period is assumed to be 15 years. Considering the weighted average cost of capital (*WACC*) of 6 % for production in highly industrialized countries [8], resulting in an annual depreciation of around 11 $\%_{FCI,}$ being in line with the literature [24,45,46]. Uncertainties associated with estimating plant costs are assessed through the variation of annual capital costs within the expected uncertainty range (−30/+50 %) [25].

The prices for continuously available electricity are estimated based on the European average price (2008—2020) for non-household electricity contracts. This value is in the same range as the constant electricity supply from renewable power in the EU derived by [47]. As there are currently no established markets for non-fossil H_2 and CO_2, the prices are estimated based on current analyses of supply costs. Thus, H_2 and CO_2 prices are varied over a wide range assigned to supply costs from different provisioning cases. The expected H_2 supply cost depends primarily on the production location and the transportation distance; variations by a factor of more than two can result. For the reference case, H_2 prices are set according to European average supply costs for power-based H_2. The expected cost range for CO_2 is even greater. While CO_2 can be provided without additional effort at advantageous point sources [48], capture costs of more than 1,000 €/t_{CO2} are currently realistic for direct air capture (DAC) [49,50]. CO_2 prices corresponding to capture costs from a point source are assumed for the reference case. However, it should be noted that the market will determine pricing more in the future and that the supply costs represent a lower price limit here.

All costs are given in euro currency and adjusted according to the chemical plant cost index (CEPCI) for 2023. The exchange rate is 1.19 US$/€ and is based on the average for the years 1999 to 2022 [55]. Additional data are provided in the supplementary material.

Table 4
Economic data and assumptions. (*ACC*: Annual capital cost, PV: Parameter variation, RC: Reference case, *WACC*: Weighted average cost of capital)

Parameter		Unit	Value	Reference
Plant related	Production capacity (total fuel product)	[kt/a]	RC: 100 | PV:10—200	[-]
	Capacity utilization[a]	[%]	RC: 70 | PV: 35—100	[-]
Capital related	*WACC* (*i*)	[%]	RC: 6 | PV: 4–15	[8,44]
	Depreciation period (*n*)	[a]	15 | 5—20	[45,46,51]
	ACC uncertainty (Factor)	[-]	0.7–1.5	[25]
Costs	H_2	[€$_{2023}$/kg]	RC: 5.0 | PV: 3.0–7.0	[44,52]
	CO_2	[€$_{2023}$/kg]	RC: 150 | PV: 0–1,000	[48–50,53]
	Electricity	[€$_{2023}$/MWh]	RC: 72 | PV: 40–190	[47,54]

[a] Capacity utilization of 70 % equals 6,132 annual full load hours.

4. Results and discussion

In this section, the process simulation results are presented first (section 4.1), serving as the basis for subsequent cost analysis. The costs for the reference cases are analyzed in section 4.2. Subsequently, the impact of the technical and economic parameter variation on kerosene production cost (*KPC*) is depicted and discussed in section 4.3.

4.1. Process simulation results

The results of the process simulations, which form the basis for calculating the variable operational expenditures and fixed capital investments, are presented as mass and electricity flows in Figs. 5 and 6. Carbon and energy flow diagrams (incl. heat streams) as well as system efficiencies under technical parameter variation, are described in the supplementary material.

4.1.1. Fischer-Tropsch pathway

For the FT pathway, a specific hydrogen demand of 0.62 t/t_K and 0.44 t/t_{TF} is observed. The CO_2 demand is 4.43t/t_K and 3.16t/t_{TF}. Considering heat integration and internal power generation, the external electricity demand (including heating requirements) amounts to 3.38 MWh/t_K and 2.41 MWh/t_{TF}, respectively. Notably, the high power demand of the electrically heated RWGS reactor is evident, which arises from both the endothermic RWGS reaction itself and the endothermic reforming of light components (primarily CH_4) from the syngas recycle and the naphtha column headstream. The water produced during the synthesis reaction is separated by condensation after the RWGS reactor and decantation from the light condensate in the cold separator after the FT synthesis.

4.1.2. Methanol pathway

The simulation of the methanol pathway shows specific hydrogen demands of 0.58 t/t_K and 0.52 t/t_{TF}. The CO_2 demand is 4.12 t/t_K and 3.74 t/t_{TF}. Steam turbines can almost supply the entire electricity required for the process by utilizing excess heat, as all main reactions in the process are exothermic. The external electricity demand is 0.06 MWh/t_K and 0.05 MWh/t_{TF}, respectively. Oligomerization allows for the direct recycling of unreacted olefins without the need for reforming. However, material losses occur due to the absence of RWGS (or further reforming options), as the resulting purge gas streams can only be used for energy recovery. The direct CO_2 conversion in methanol synthesis leads to low conversion rates, resulting in large mass flows and corresponding sizing requirements in the synthesis loop.

The higher kerosene selectivity of the MeOH pathway compared to the FT pathway results primarily from the larger monomer building blocks (ethene, propene), which can form hydrocarbons in the kerosene fraction with fewer chain growth reactions (lower chain growth probability). This is further supported by light fractions recycled directly without breaking the already-formed chains (supplementary material,

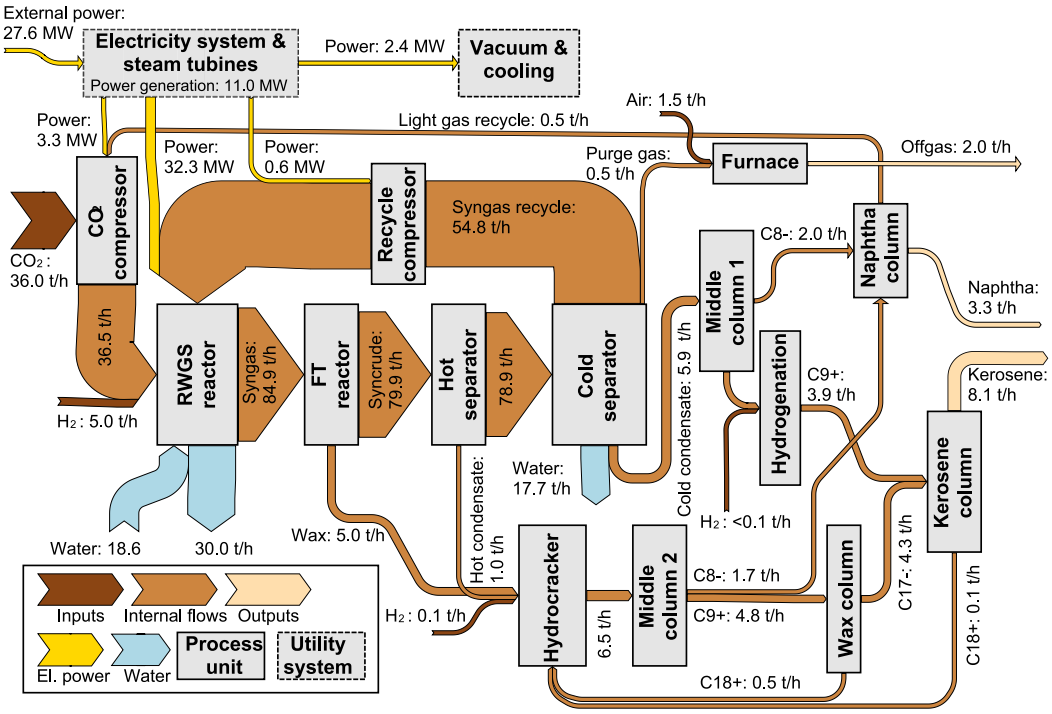

Fig. 5. Mass and electricity flows of the Fischer-Tropsch pathway. (Diagram represents the reference case; Heat flows are not shown for reasons of visual clarity. Power flows below 0.1 MW not shown; FT. Fischer-Tropsch, RWGS: Reverse water–gas shift)

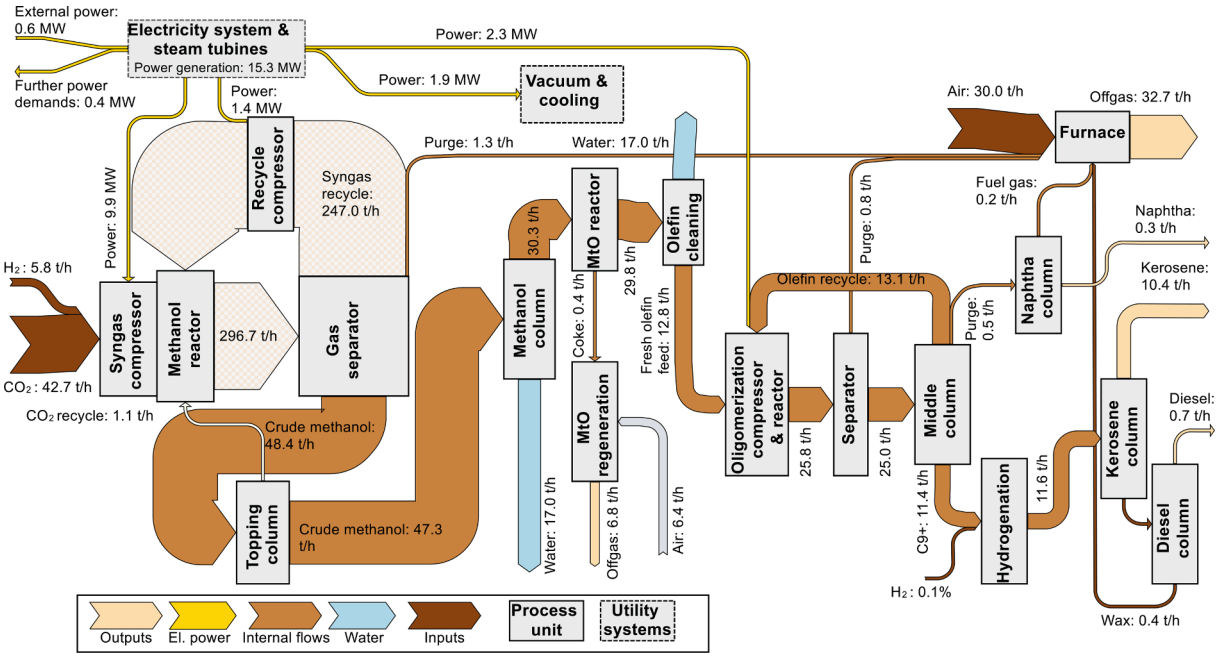

Fig. 6. Mass and electricity flows of the methanol pathway. (Diagram represents the reference case; Heat flows are not shown for reasons of visual clarity. Power flows below 0.1 MW not shown; MtO: Methanol-to-olefins)

section 4.3).

4.2. Production cost

Fig. 7 depicts the kerosene production costs of both pathways (reference case) for both cost allocation methods. The left side of the figure (KPC_K) represents the allocation of costs solely to the kerosene fraction without accounting for by-product revenues, therefore indicating an upper cost limit. The right side represents the equal allocation of costs across all fuel products (naphtha, kerosene, diesel fraction), indicating a lower cost limit (KPC_{TF}). The proportions of the individual cost components shown are equal within both allocations. Electricity production from internal heat conversion is offset against the external electricity supply.

In the reference case, the FT pathway yields kerosene production costs between 3,630 and 5,070 €/t, depending on the allocation method/the by-product revenues, respectively. For the MeOH pathway, costs are within a smaller range of 4,240 to 4,660 €/t. The costs of both

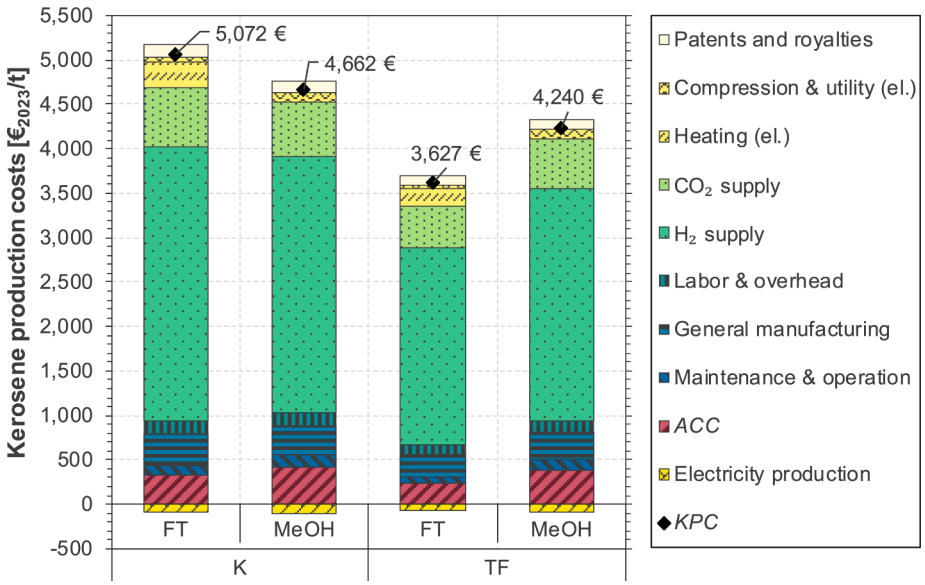

Fig. 7. Kerosene production costs of the Fischer-Tropsch and methanol pathway in the reference case. (K: Kerosene allocation, TF: Total fuel allocation, FT: Fischer-Tropsch, MeOH: Methanol, *ACC*: Annual capital cost, *KPC*: Kerosene production cost)

pathways are dominated by the costs of H_2 (FT: 61 %, MeOH 62 %) and CO_2 supply (both 13 %). The shares of the remaining cost components are distributed relatively evenly across the kerosene production costs. The major difference between the cost distribution of the FT and MeOH pathway lies in the electricity cost. The FT pathway requires significantly more electricity (mainly for RWGS heating) than is supplied by internal heat conversion. In contrast, the electricity demand and generation are almost equal within the MeOH pathway. The fixed capital investments, resulting from the major equipment estimate used, are 150 M€ for the FT pathway and 240 M€ for the MeOH pathway (see supplementary material). The higher fixed capital investments required for the MeOH pathway result mainly from the larger synthesis loop and the higher pressure level of the methanol synthesis. Therefore, the resulting share of annual capital cost is also slightly higher for the MeOH pathway (9 %) than for the FT pathway(7 %).

Comparing both pathways' kerosene production costs, the kerosene production via the MeOH pathway results in lower costs when no revenues from naphtha or diesel are considered (KPC_K). However, considering all fuel fractions as (equally) valuable products, the FT pathway enables significantly lower production costs (KPC_{TF}). The first result is caused by the high kerosene selectivity of the olefin oligomerization (MeOH pathway). In contrast, the advantage of the FT pathway regarding KPC_{TF} is due to the low material losses and, thus, the higher total fuel production.

Fig. 8 depicts the kerosene production cost over varying by-product revenues (*BPR*). Both of the above-described allocations can be found in the figure.

KPC_K occur at a by-product revenue of 0 €/t_{BP}. KPC_{TF} are located where the kerosene production costs are equal to the by-product revenues. Due to the larger by-product quantity, the kerosene production costs of the FT pathway in the analyzed plant concepts are significantly more dependent on the by-product revenues. Equal kerosene production costs for both pathways (*KPC eq.*) occur at a by-product revenue of around 1,370 €/t_{BP}. The respective kerosene production costs are 4,530 €/t. Below this value, the MeOH pathway enables lower kerosene production costs; at higher by-product revenues, the FT pathway enables cheaper kerosene production. In other words, the MeOH pathway would be economically beneficial only for kerosene market prices, which are 3.3 times higher than naphtha or diesel prices. Optimizing the process concepts toward maximized naphtha or diesel production would be economically beneficial if higher revenues are achieved for the by-products than for kerosene.

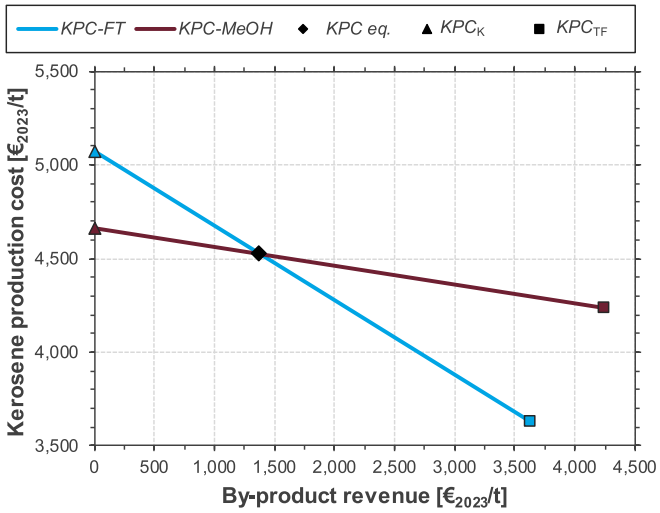

Fig. 8. Kerosene production cost of the Fischer-Tropsch and methanol pathway under varying by-product revenues. (FT: Fischer-Tropsch pathway, MeOH: Methanol pathway, eq.: equal, *KPC*: Kerosene production cost, KPC_K: Kerosene production cost from kerosene allocation, KPC_{TF}: Kerosene production cost from total fuel allocation)

4.3. Parameter variation

In simulation-based techno-economic analyses, the cost calculation results strongly depend on the underlying technical and economic concepts and assumptions. The variation of key parameters is analyzed below to show the respective impacts on kerosene production costs and to determine realistic cost ranges for power-based fuel production.

4.4. Technical parameters

The results of the technical parameter variation are shown in Fig. 9. The solid lines represent the kerosene allocation (KPC_K), i.e., excluding by-product revenues, and the dashed lines show the cost allocation to the total fuel fraction (KPC_{TF}). In the FT pathway, the chain growth

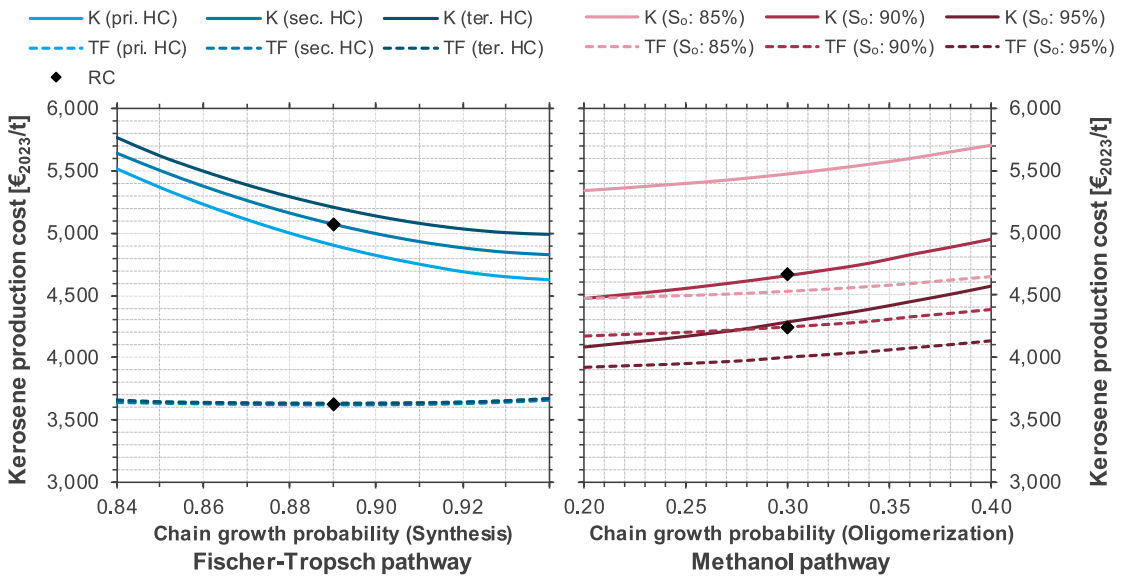

Fig. 9. Kerosene production cost under technical parameter variation. (K: Kerosene allocation, TF: Total fuel allocation, S_O: Olefin selectivity pri.: primary, sec.: secondary, ter.: tertiary, HC: Hydrocracking, RC: Reference case)

probability within the FT reactor and the degree of hydrocracking, i.e., single (pri.), double (sec.), and triple (tert.) cracking possibility per reactor pass, are varied as higher-level process parameters (see section 3.1). The diagram indicates that both parameters have almost no impact in the varied range when costs are allocated to the total fuel product – meaning KPC_{TF} stay nearly constant. This is due to the fact that while the relative proportions of the fuel fractions shift, the overall quantity of fuel produced remains nearly constant. However, energy demand and wax distillation costs increase slightly with increasing chain growth probability, while the energy demand of the RWGS reactor increases with decreasing chain growth probability (increasing recycling of light gases). This leads to minimal KPC_{TF} at chain growth probabilities around 0.9. Mild hydrocracking (pri. HC) and high chain growth probabilities increase the kerosene fraction, reducing kerosene production costs within kerosene allocation (KPC_K).

Within the MeOH pathway, KPC_K and KPC_{TF} are strongly affected by the varied parameters of olefin selectivity (S_O) and oligomerization chain growth probability since total fuel and kerosene yield change significantly. Generally, low chain growth probabilities and high olefin selectivities positively affect technical efficiencies and kerosene production costs. A comparison of the economic results with the technical results (supplementary material) reveals a strong correlation between the production costs and the process efficiencies. As in the FT pathway, the KPC_{TF} are less affected by the chain growth probability as this parameter mainly changes the proportions of fuel fractions. However, with high probabilities of chain growth, an increasing wax fraction occurs, reducing the overall amount of fuel produced. Low chain growth probabilities increase the kerosene selectivity of the overall process as less diesel and waxes are produced. The increasing naphtha fraction is recycled, thus increasing the energy input and dimensioning of the oligomerization loop. However, this is more than compensated for by the higher efficiency of the process in terms of kerosene production. A higher olefin selectivity directly reduces the amount of purge gas and increases the overall process efficiency.

The methanol pathway shows lower kerosene production costs over a wide range of parameter variations when no revenues for naphtha or diesel are considered (KPC_K). This is due to the higher kerosene selectivity compared to the FT pathway, making by-product revenue less critical. However, cost allocation to all fuel products (KPC_{TF}) shows lower production costs within the FT pathway that cannot be reached by the methanol pathway, even under the most favorable assumptions. Within the FT pathway, the KPC_K varies from 4,630 to 5,770 €/t (RC: 5,070 €/t; −9 %, +14 %). KPC_{TF} change is minimal from 3,630 to 3,670 €/t (RC: 3,630 €/t; −0 %, +1 %). The variation is much stronger in the MeOH pathway, where KPC_K varies from 4,080 to 5,710 €/t (RC: 4,660 €/t; −12 %, +22 %) and KPC_{TF} changes from 3,920 – 4,640 €/t (RC: 4,240 €/t; −8 % +10 %).

4.5. Economic parameters

Fig. 10 shows the kerosene production cost under the variation of four economic parameters. The solid lines represent the kerosene allocation (KPC_K), and the dashed lines show the total fuel allocation (KPC_{TF}). The influence of the economic parameters analyzed here on the MeOH pathway is slightly more significant, as the fixed capital investments are higher. However, within the expected parameter ranges, the MeOH pathway always enables lower kerosene production costs when no by-product revenues are assumed (KPC_K), while the FT pathway allows for lower kerosene production costs when all fuel fractions are assumed to have the same value (KPC_{TF}).

4.5.1. Weighted average cost of capital

Within the FT pathway, the KPC_K varies from 5,020 to 5,320 €/t (RC: 5,070 €/t; −1 %, +5 %). The KPC_{TF} varies between 3,590 and 3,800 €/t (RC: 3,630 €/t; −1 %, +5 %). KPC_K in the MeOH pathway varies from 4,600 to 4,970 €/t (RC: 4,660 €/t; −1 %, +7 %), and KPC_{TF} changes between 4,190 and 4,520 €/t (RC: 4,240 €/t; −1 % +7 %). The weighted average cost of capital depends on plant location and numerous further factors. However, the *WACC* has a minor impact on kerosene production costs since annual capital costs only contribute a small fraction of overall costs. This parameter is typically much more important for very capital-intensive production processes (e.g., electricity generation, water-electrolyzer).

4.5.2. Depreciation period

Within the FT pathway, the KPC_K varies from 5,030 to 5,470 €/t (RC: 5,070 €/t; −1 %, +8 %), and the KPC_{TF} ranges from 3,590 to 3,910 €/t (RC: 3,630 €/t; −1 %, +8 %). Again, the MeOH pathway is slightly more affected, with KPC_K between 4,600 and 5,170 €/t (RC: 4,660 €/t; −1 %, +11 %) and KPC_{TF} varying from 4,190 to 4,700 €/t (RC: 4,240 €/t; −1 %, +11 %). The length of the period assumed for investment depreciation has a non-linear influence on the kerosene production

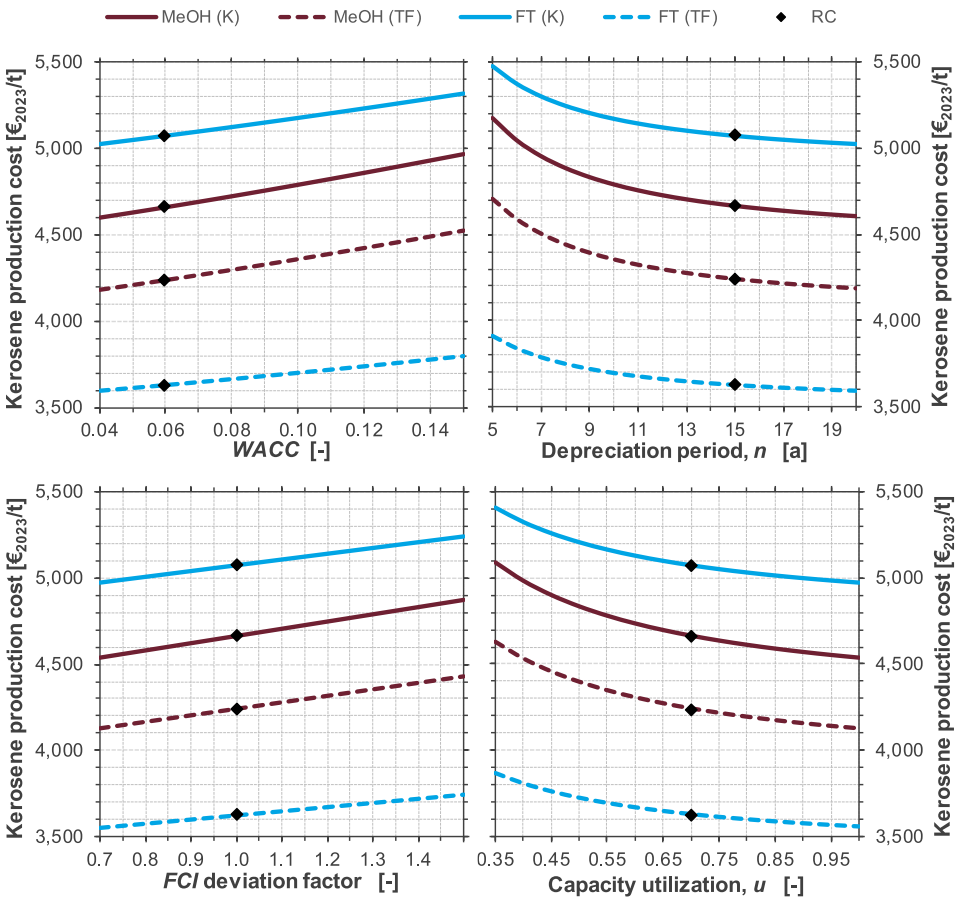

Fig. 10. Kerosene production costs under economic parameter variation. (FT: Fischer-Tropsch pathway, MeOH: Methanol pathway, K: Kerosene allocation, TF: Total fuel allocation, RC: Reference case, WACC: Weighted average cost of capital, FCI: Fixed capital investment)

costs. Considerable cost increases particularly occur for amortization periods of less than ten years. For amortization periods longer than ten years, the effect is limited due to the relatively small share of annual capital cost within the kerosene production cost.

4.5.3. Annual capital cost

The major equipment estimate method used for fixed capital investment calculation, by definition, has an accuracy of −30/+50 %, which is reflected here using the fixed capital investment (*FCI*) deviation factor. The kerosene production costs change linearly and relatively flat. Within the FT pathway, KPC_K increase from 4,970 to 5,240 €/t (RC: 5,070 €/t; −2 %, +3 %), and the KPC_{TF} increase from 3,560 to 3,750 €/t (RC: 3,630 €/t; −2 %, +3 %). Due to the higher fixed capital investment required for the MeOH pathway, KPC_K and KPC_{TF} change slightly stronger from 4,540 to 4,870 €/t (RC: 4,660 €/t; −3 %, +5 %) and 4,120 to 4,430 €/t (RC: 4,240 €/t; −3 %, +5 %) respectively.

4.5.4. Capacity utilization

Capacity utilization is decisive for the amount of product produced to which all fixed costs are related. Accordingly, the impact on kerosene production cost is non-linear and increases in particular at low utilizations. Within the FT pathway, KPC_K and KPC_{TF} can be decreased to 4,970 and 3,560 €/t (−2 % of RC) when nominal load production can be achieved over the entire year. However, the H_2 supply from fluctuating power-based electrolysis might only be made available constantly at much higher prices, making lower capacity utilization economically favorable at certain times. A lower utilization at constant feedstock prices can increase the KPC_K and KPC_{TF} up to 5,410 €/t and 3,870 €/t (+7 %). The same applies to the MeOH pathway, where KPC_K varies from 4,540 to 5,090 €/t (RC: 4,660 €/t; −3 %, +9 %), and KPC_{TF} varies from 4,120 – 4,630 €/t (RC: 4,240 €/t; −3 % +9 %). The influences of feedstock prices are depicted in Fig. 11.

4.5.5. H_2 price

Within the assumed H_2 price range, KPC_K and KPC_{TF} vary between ± 24 % (FT) and ± 25 % (MeOH) of the reference case cost. For the FT pathway, the KPC_K ranges from 3,830 to 6,310 €/t and the KPC_{TF} from 2,740 to 4,510 €/t. Within the MeOH pathway, the cost ranges from 3,510 to 5,810 €/t and 3,190 to 5,290 €/t, respectively. Power-based H_2 production is expensive due to the high electricity demand and the high capital investments for the electrolyzer. Furthermore, a significant amount of H_2 is required since it is the main energetic input within the analyzed process pathways. Accordingly, the H_2 price has a high impact on the *KPC*.

4.5.6. CO_2 price

Even if the specific prices of H_2 are significantly higher than those of CO_2, the CO_2 price equally influences the kerosene production costs. This is due, on the one hand, to the (mass-related) higher demand for CO_2 and, on the other hand, to the potentially vast price range depending on the supply option and the market development. Possible cost reductions, for example, if pure CO_2 is produced as a waste product without alternative use (0 €/t_{CO2}), can lead to reduced costs of 13 % compared to the reference cases. In contrast, CO_2 prices that refer to the provision costs via DAC, currently lying around 1,000 €/t_{CO2}, increase the kerosene production cost by 74 % (FT) and 75 % (MeOH) compared to the reference case. The KPC_K in the FT pathway ranges from 4,410 to 8,830 €/t. The KPC_{TF} increases from 3,150 – 6,320 €/t. Within the MeOH pathway, KPC_K and KPC_{TF} vary from 4,040 to 8,160 €/t and 3,680 – 7,420 €/t, respectively.

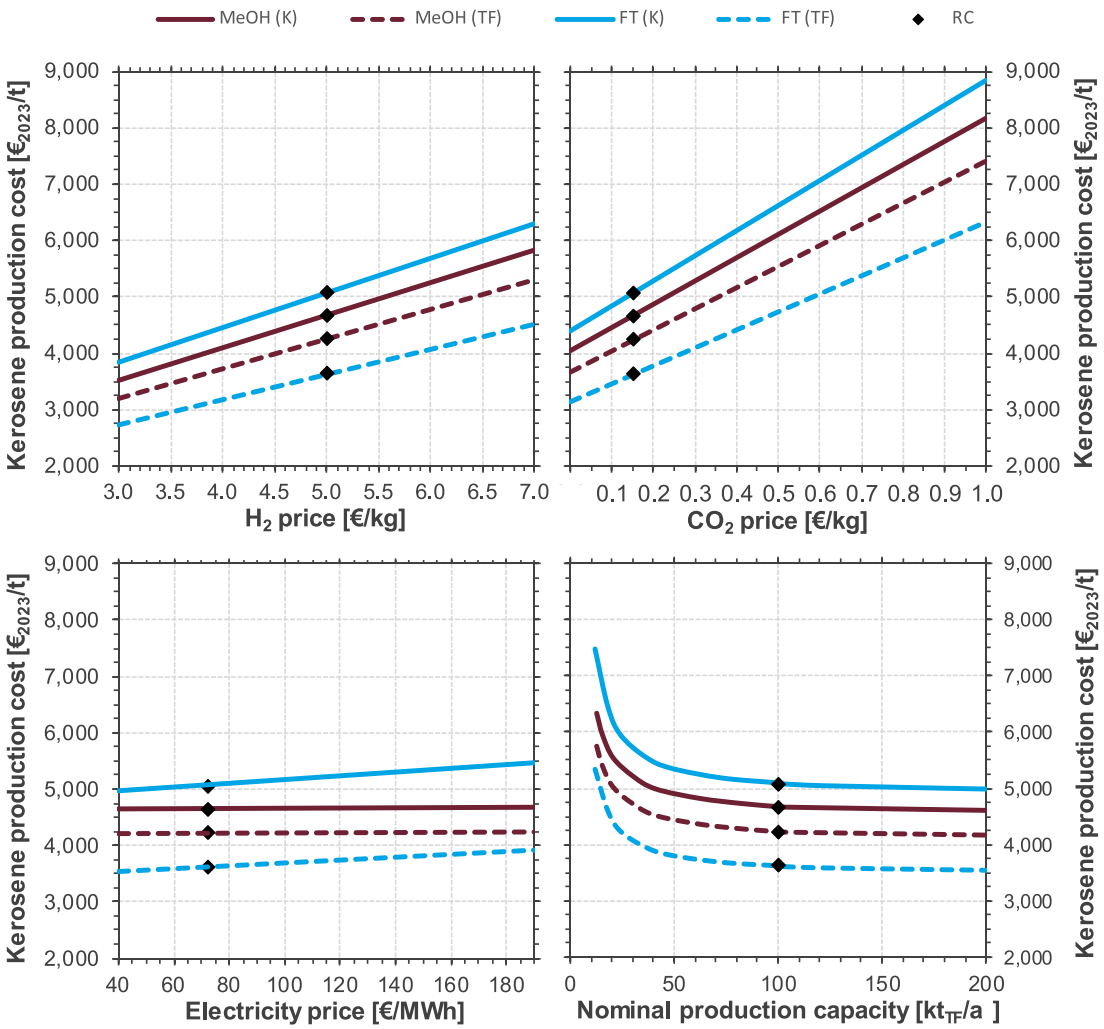

Fig. 11. Kerosene production cost under feedstock price and nominal production capacity variation. (FT: Fischer-Tropsch pathway, MeOH: Methanol pathway, K: Kerosene allocation, TF: Total fuel allocation, RC: Reference case)

4.5.7. *Electricity price*

The influence of electricity prices affects both pathways in very different ways. While MeOH-based production requires almost no external electricity and is therefore widely independent from the electricity price, the variation carried out here results in changes between −2 and + 8 % (KPC_K 4,960 to 5,470 €/t; KPC_{TF} 3,550 to 3,910 €/t) in the FT pathway. At an electricity price of around 330 €/MWh and higher, the MeOH pathway would be cheaper even if the costs are allocated to total fuel product (KPC_{TF}). However, such high electricity prices seem unlikely for industrial customers.

4.5.8. *Nominal plant capacity*

The nominal plant capacity variation depicts the effects of scale on the kerosene production cost. A strong effect of the realized plant sizes can be seen between 10 and 50 kt_{TF}/a. Decreasing equipment size and thus increasing specific equipment costs lead to a significant rise in the share of annual capital costs, particularly for plant capacities below 30 kt_{TF}/a. In contrast, between 100 and 200 kt_{TF}/a, further cost reductions are minimal, among others, as some components reach standard industrial equipment's capacity limits. While in both production cases, only minor cost reductions can be expected through further upscaling (based on the cost method used here, 3 % (FT) to 2 % (MeOH)), the costs for very small-scale systems can lead to production cost increases clearly above 30 % compared to the reference case.

5. Summary and discussion

The different influences from parameter variation on the kerosene production costs are depicted in Fig. 12. The left diagram depicts the kerosene production costs excluding by-product revenues (KPC_K), while the right diagram presents the costs derived by total fuel allocation (KPC_{TF}). Depending on the allocation method/by-product value and the assumed parameters, the kerosene production costs are predominantly between 3,500 and 5,500 €/t. The figure shows that H_2 and CO_2 prices determine kerosene production costs significantly within both pathways; thus, price changes lead to high cost variations. In particular, CO_2 prices equivalent to the current supply costs via direct air capture can nearly double kerosene production costs compared to applying CO_2 supply cost from point sources. The plant's production capacity also significantly affects kerosene production costs within 10 to 50 kt_{TF}/a range. Here, economy-of-scale effects result in a significant cost increase for small-scale production facilities.

Technical parameter variations considerably influence the kerosene production cost of both pathways when no by-product revenue is considered (KPC_K). However, when naphtha, kerosene, and diesel are of equal value (total fuel cost allocation, KPC_{TF}), only the MeOH pathway

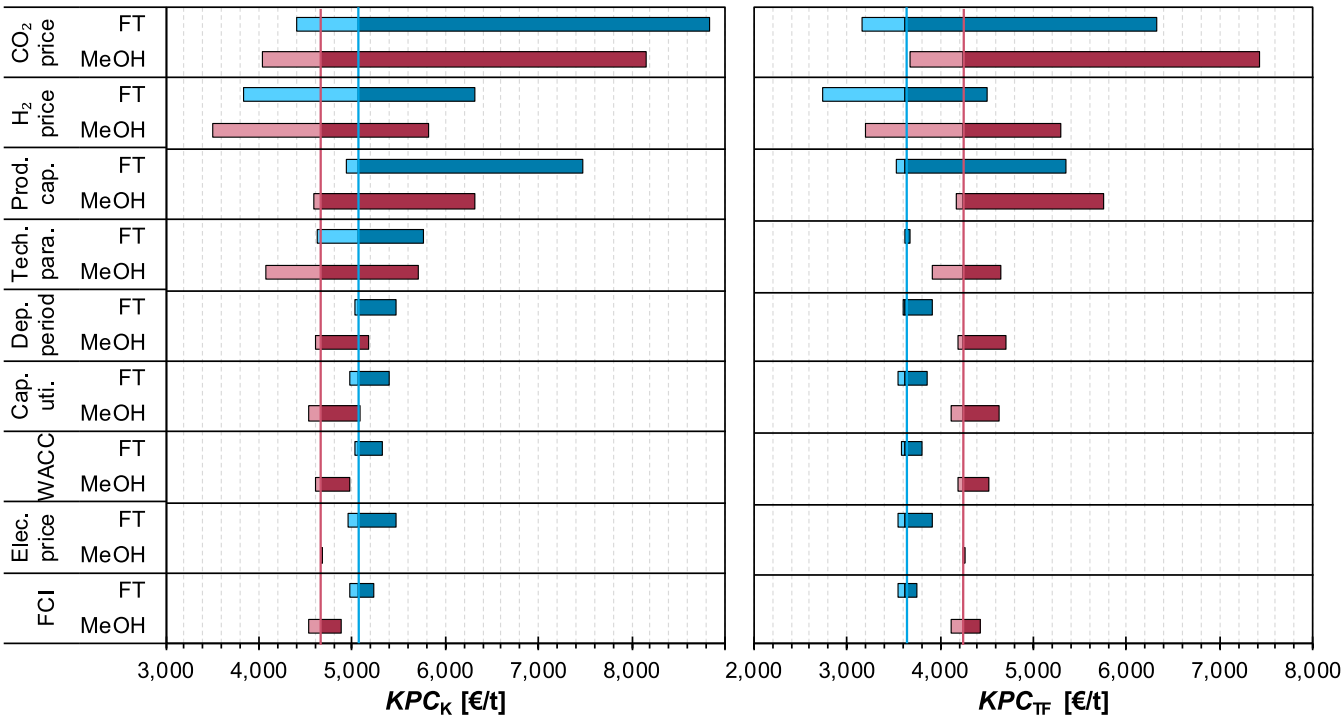

Fig. 12. Comparison of parameter variation impacts on kerosene production cost. (FT: Fischer-Tropsch pathway; MeOH: Methanol pathway; KPC_K: Kerosene production cost based on kerosene allocation; KPC_{TF}: Kerosene production cost based on total fuel allocation; Tech. para.: Technical parameter; *WACC*: Weighted average cost of capital; Dep.: Depreciation; *FCI*: Fixed capital investment, Cap. uti.: Capacity utilization; Elec.: Electricity; Prod. cap.: Production capacity)

is affected by technical parameter variation. The economic parameters varied (depreciation period, weighted average cost of capital, fixed capital investment, capacity utilization) show a lower effect on kerosene production cost, with the MeOH pathway being slightly more sensitive due to its higher plant costs. The electricity price only affects the FT pathway since the MeOH pathway has hardly any external electricity demand. However, lower KPC_{TF} only result for the MeOH pathway when applying very high electricity prices of 330 €/MWh and more.

Concerning the technical parameters, the MeOH pathway shows more significant uncertainties than the FT pathway. Based on the utilization of fossil syngas, the FT pathway is commercially used for the synthetic production of various fuels and has been extensively studied and described in the literature [35,36,56–59]. The chain growth probability and hydrocracking intensity can be adjusted through appropriate catalysts and process conditions, making a further maximization of the kerosene fraction (as shown in the parameter variation) feasible. In contrast, there is significantly less data available in the literature for methanol-based kerosene production, while various process concepts are proposed, particularly regarding the combination of dehydration and oligomerization [21,22,60]. As a result, the modeling is based on a much smaller data set compared to the FT pathway, leading to greater uncertainties. Therefore, the results from the parameter variation rather represent an uncertainty range surrounding the reference case.

Further uncertainties exist about calculating plant costs (fixed capital investment) using the module costing technique. Although this method has relatively high accuracy (−30/+50 %), corresponding functions are not available in the literature for all types of equipment and process conditions, which can result in larger deviations. The limited validity range of the functions severely restricts a statement beyond the varied size range. Even if the cost reduction slowly flattens out between capacities of 100 and 200 kt_{TF}/a, further cost reductions can potentially occur in larger-scale projects, even if this cannot be evaluated with the cost functions used here [35]. Since many of the fixed operational expenditures are calculated on the basis of fixed capital investments, such uncertainties also apply to parts of these costs.

6. Conclusion

The successful market integration of power-based aviation fuels necessitates a thorough understanding of the cost structure and the key factors influencing kerosene production costs. This study presents a comprehensive cost analysis of kerosene production from power-based syngas, comparing two different plant concepts, one using the Fischer-Tropsch synthesis and hydrotreatment, the other applying direct methanol synthesis with downstream dehydration and oligomerization. Two cost allocation methods are applied to address uncertainties associated with unpredictable by-product revenues. Allocating costs solely to the kerosene fraction, without considering by-product revenues, establishes the upper cost limit (KPC_K), while allocating costs across the total fuel fraction, resulting in equal production costs for all fuel products, defines the lower cost boundary (KPC_{TF}). Novel findings result from the detailed comparison of the process pathways based on the same framework conditions and extensive parameter variation.

The main conclusions that can be drawn with regard to the analyzed process concepts in the reference case can be summarized as follows:

- Applying the above-mentioned cost allocations reveals a significantly lower impact of achievable naphtha and diesel revenues on the kerosene production cost in the MeOH pathway due to its high kerosene selectivity. In contrast, kerosene production costs in the FT pathway are more sensitive to variations in by-product revenues, ranging from 3,630 to 5,070 €/t, while in the MeOH pathway, by-product price-related cost changes range from 4,240 to 4,660 €/t.
- Due to its high material efficiency, the FT pathway becomes advantageous compared to the MeOH pathway already at by-product revenues equivalent to 30 % (1,370 €/t) of the associated kerosene production costs (4,530 €/t); i.e., kerosene must be 3.3 times more valuable than naphtha and diesel to result in lower kerosene production costs for the MeOH pathway.

Analyzing the parameter variations yields the following results for

the plant concepts investigated here:

- Variations in technical parameters have a more significant impact on the MeOH pathway than on the FT pathway. Both, a more limited availability of process modeling data and a greater sensitivity to the varied parameters cause a higher uncertainty for the MeOH pathway – the KPC_K ranges from −12 to + 22 %, and the KPC_{TF} from −8 to + 10 %. Within the FT pathway, KPC_K and KPC_{TF} vary only by −8 to + 13 % and 0 to 1 %, respectively.
- In general, *KPCs* strongly correlate with technical efficiencies, with changes in plant investment (e.g., due to larger equipment dimensions) having only a minor effect on overall costs.
- The H_2 and CO_2 prices have the most significant influence on kerosene production costs. Lowering the costs of H_2 production can reduce kerosene production costs by up to 25 % (within the expected H_2 price range). CO_2 price, especially in the range of current DAC costs, can increase kerosene production costs by up to 75 % compared to price levels referring to point source carbon capture costs.

Since a broad data basis is already available for modeling the industrially established FT pathway and the higher-level process parameters (chain growth probability, hydrocracking intensity) are largely adjustable, the parameter variation results can be considered as a feasible optimization range. The MeOH pathway has significantly greater uncertainties due to the lack of industrial validation and the smaller data basis. Therefore, the results from the parameter variation primarily represent the uncertainties rather than the practically achievable optimization range.

In conclusion, based on the analyzed kerosene production costs, which primarily range between 3,500 and 5,500 €/t, power-based aviation fuels are expected to be significantly more expensive than most biomass-based kerosene alternatives. The primary cost drivers are found upstream of the synthesis process, i.e., H_2 production and potentially CO_2 supply. Thus, the efficiency of feedstock utilization becomes even more important. This suggests that extensive measures to enhance feedstock conversion efficiency could be economically viable despite increasing plant complexity. Therefore, further studies are needed to develop and optimize concepts with maximized feedstock utilization and kerosene yield.

CRediT authorship contribution statement

Stefan Bube: Writing – original draft, Visualization, Software, Methodology, Investigation, Formal analysis, Conceptualization. **Steffen Voß:** Validation, Software, Methodology. **Gunnar Quante:** Writing – review & editing, Visualization. **Martin Kaltschmitt:** Writing – review & editing, Supervision.

Declaration of competing interest

The authors declare that they have no known competing financial interests or personal relationships that could have appeared to influence the work reported in this paper.

Appendix A. Supplementary data

Supplementary data to this article can be found online at https://doi.org/10.1016/j.fuel.2024.133901.

Data availability

Data will be made available on request.

References

[1] International Air Transport Association. Resolution on the industry's commitment to reach net zero carbon emissions by 2050: Press Release No: 66; 2021.
[2] International Civil Aviation Organization. Resolution A41-21.: Consolidated statement of continuing ICAO policies and practices related to environmental protection - Climate change. Montréal; 2022.
[3] Quante G, Bullerdiek N, Bube S, Neuling U, Kaltschmitt M. Renewable fuel options for aviation – A System-Wide comparison of Drop-In and non Drop-In fuel options. Fuel 2023;333:126269. https://doi.org/10.1016/j.fuel.2022.126269.
[4] Gong A, Verstraete D. Fuel cell propulsion in small fixed-wing unmanned aerial vehicles: Current status and research needs. Int J Hydrogen Energy 2017;42(33):21311–33. https://doi.org/10.1016/j.ijhydene.2017.06.148.
[5] Focus Roland Berger. Hydrogen: A future fuel for aviation?; 2020.
[6] Bullerdiek N. Kerosinoptionen auf Basis regenerativer Energien im internationalen Luftverkehr: Identifikation, Analyse und Bewertung kosteneffizienter und klimazielkompatibler Integrationspfade [Dissertation]. Hamburg: Technische Universität Hamburg (TUHH); 2024.
[7] Bube S, Bullerdiek N, Voß S, Kaltschmitt M. Kerosene production from power-based syngas – A technical comparison of the Fischer-Tropsch and methanol pathway. Fuel 2024;366:131269. https://doi.org/10.1016/j.fuel.2024.131269.
[8] Agora Verkehrswende and PtX Hub. Defossilising aviation with e-SAF: An introduction to technologies, policies, and markets for sustainable aviation fuels; 2024.
[9] Drünert S, Neuling U, Zitscher T, Kaltschmitt M. Power-to-Liquid fuels for aviation – Processes, resources and supply potential under German conditions. Appl Energy 2020;277:115578. https://doi.org/10.1016/j.apenergy.2020.115578.
[10] Neuling U, Kaltschmitt M. Techno-economic and environmental analysis of aviation biofuels. Fuel Process Technol 2018;171:54–69. https://doi.org/10.1016/j.fuproc.2017.09.022.
[11] Making Net-Zero Aviation Possible 2022.
[12] Voß S, Bube S, Kaltschmitt M. Hybrid Biomass- and Electricity-Based Kerosene Production—A Techno-Economic Analysis. Energy Fuels 2024;38(6):5263–78. https://doi.org/10.1021/acs.energyfuels.3c04876.
[13] Schemme S, Breuer JL, Köller M, Meschede S, Walman F, Samsun RC, et al. H2-based synthetic fuels: A techno-economic comparison of alcohol, ether and hydrocarbon production. Int J Hydrogen Energy 2020;45(8):5395–414. https://doi.org/10.1016/j.ijhydene.2019.05.028.
[14] Rojas-Michaga MF, Michailos S, Cardozo E, Akram M, Hughes KJ, Ingham D, et al. Sustainable aviation fuel (SAF) production through power-to-liquid (PtL): A combined techno-economic and life cycle assessment. Energ Conver Manage 2023;292:117427. https://doi.org/10.1016/j.enconman.2023.117427.
[15] König DH. Techno-ökonomische Prozessbewertung der Herstellung synthetischen Flugturbinentreibstoffes aus CO2 und H2. Dissertation 2016.
[16] Seymour K, Held M, Stolz B, Georges G, Boulouchos K. Future costs of power-to-liquid sustainable aviation fuels produced from hybrid solar PV-wind plants in Europe. Sustainable Energy Fuels 2024;8(4):811–25. https://doi.org/10.1039/D3SE00978E.
[17] Colelli L, Segneri V, Bassano C, Vilardi G. E-fuels, technical and economic analysis of the production of synthetic kerosene precursor as sustainable aviation fuel. Energ Conver Manage 2023;288:117165. https://doi.org/10.1016/j.enconman.2023.117165.
[18] Raab M, Dietrich R-U. Techno-economic assessment of different aviation fuel supply pathways including LH2 and LCH4 and the influence of the carbon source. Energ Conver Manage 2023;293:117483. https://doi.org/10.1016/j.enconman.2023.117483.
[19] Meurer A, Jochem P, Kern J. Decentralised production of e-fuels for aviation: implications and trade-offs of a targeted small-scale production of sustainable aviation fuel based on Fischer–Tropsch synthesis. Sustainable Energy Fuels 2024;8(4):752–65. https://doi.org/10.1039/D3SE01156A.
[20] Peacock J, Cooper R, Waller N, Richardson G. Decarbonising aviation at scale through synthesis of sustainable e-fuel: A techno-economic assessment. Int J Hydrogen Energy 2024;50:869–90. https://doi.org/10.1016/j.ijhydene.2023.09.094.
[21] Atsonios K, Li J, Inglezakis VJ. Process analysis and comparative assessment of advanced thermochemical pathways for e-kerosene production. Energy 2023;278:127868. https://doi.org/10.1016/j.energy.2023.127868.
[22] Hirunsit P, Senocrate A, Gómez-Camacho CE, Kiefer F. From CO 2 to Sustainable Aviation Fuel: Navigating the Technology Landscape. ACS Sustainable Chem Eng 2024. https://doi.org/10.1021/acssuschemeng.4c03939.
[23] Schemme S. Techno-ökonomische Bewertung von Verfahren zur Herstellung von Kraftstoffen aus H2 und CO2: Dissertation. Jülich: Energie & Umwelt / Energy & Environment; 2020.
[24] Turton R. Analysis, synthesis, and design of chemical processes, fifth edition. Boston [etc.]: Prentice Hall; op. 2018.
[25] Association for the Advancement of Cost Engineering. COST ESTIMATE CLASSIFICATION SYSTEM-AS APPLIED IN ENGINEERING, PROCUREMENT, AND CONSTRUCTION FOR THE PROCESS INDUSTRIES: AACE® International Recommended Practice No. 18R-97. TCM Framework: 7.3 – Cost Estimating and Budgeting.
[26] Buttler A, Spliethoff H. Current status of water electrolysis for energy storage, grid balancing and sector coupling via power-to-gas and power-to-liquids: A review. Renew Sustain Energy Rev 2018;82:2440–54. https://doi.org/10.1016/j.rser.2017.09.003.

[27] Siemens Energy. Silyzer 300: The next paradigm of PEM electrolysis. [January 18, 2024]; Available from: https://assets.siemens-energy.com/siemens/assets/api/uuid:a193b68f-7ab4-4536-abe2-c23e01d0b526/datasheet-silyzer300.pdf.
[28] Porter RT, Fairweather M, Pourkashanian M, Woolley RM. The range and level of impurities in CO2 streams from different carbon capture sources. Int J Greenhouse Gas Control 2015;36:161–74. https://doi.org/10.1016/j.ijggc.2015.02.016.
[29] Kadlecek D. Methanol to Jet (MTJ): ASTM D02.0J AC724 Task Force. [July 17, 2024]; Available from: www.caafi.org/resources/pdf/Methanol-to-Jet_CAAFI_Kadlecek_07_25_2023.pdf.
[30] Reddy C, Rangaiah GP. Retrofit of Vacuum Systems in Process Industries. In: Rangaiah GP, editor. Chemical Process Retrofitting and Revamping. Wiley; 2016. p. 317–46.
[31] Adelung S, Dietrich R-U. Impact of the reverse water-gas shift operating conditions on the Power-to-Liquid fuel production cost. Fuel 2022;317:123440. https://doi.org/10.1016/j.fuel.2022.123440.
[32] Wesenberg MH. Gas heated steam reformer modelling. Trondheim: NTNU; 2006.
[33] Grabke HJ. Metal dusting. Mater Corros 2003;54(10):736–46. https://doi.org/10.1002/maco.200303729.
[34] Hiller H, Reimert R, Marschner F, Renner H-J, Boll W, Supp E et al. Gas Production. In: Ullmann's Encyclopedia of Industrial Chemistry.
[35] Dieterich V, Buttler A, Hanel A, Spliethoff H, Fendt S. Power-to-liquid via synthesis of methanol, DME or Fischer–Tropsch-fuels: a review. Energy Environ Sci 2020;13(10):3207–52. https://doi.org/10.1039/D0EE01187H.
[36] de Klerk A. Fischer-Tropsch refining. Weinheim: Wiley-VCH; 2011.
[37] Bube S, Hofbauer H, Kaltschmitt M, Klemm M, Neuling U, Voß S, et al. Synthese- und Weiterverarbeitungsverfahren. In: Kaltschmitt M, Hofbauer H, Lenz V, editors. Energie aus Biomasse. Wiesbaden: Springer Fachmedien Wiesbaden; 2024. p. 1011–99.
[38] Hamelinck C, Faaij A, Denuil H, Boerrigter H. Production of FT transportation fuels from biomass; technical options, process analysis and optimisation, and development potential. Energy 2004;29(11):1743–71. https://doi.org/10.1016/j.energy.2004.01.002.
[39] Bouchy C, Hastoy G, Guillon E, Martens JA. Fischer-Tropsch Waxes Upgrading via Hydrocracking and Selective Hydroisomerization. Oil & Gas Science and Technology - Rev IFP 2009;64(1):91–112. https://doi.org/10.2516/ogst/2008047.
[40] Babu BH, Lee M, Hwang DW, Kim Y, Chae H-J. An integrated process for production of jet-fuel range olefins from ethylene using Ni-AlSBA-15 and Amberlyst-35 catalysts. Appl Catal A 2017;530:48–55. https://doi.org/10.1016/j.apcata.2016.11.020.
[41] Lacarriere A, Robin J, Swierczyński D, Finiels A, Fajula F, Luck F, et al. Distillate-range products from non-oil-based sources by catalytic cascade reactions. ChemSusChem 2012;5(9):1787–92. https://doi.org/10.1002/cssc.201200092.
[42] Gogate MR. Methanol-to-olefins process technology: current status and future prospects. Pet Sci Technol 2019;37(5):559–65. https://doi.org/10.1080/10916466.2018.1555589.
[43] Liu Hongxing, Xie Zaiku, Zhao Guoliang. The Progress of SINOPEC Methanol-To-Olefins (S-MTO) Technology: Shanghai Research Institute of Petrochemical Technology SINOPEC, China. In: October 9 - 11, 2013, Dresden, Germany.
[44] Sens L, Piguel Y, Neuling U, Timmerberg S, Wilbrand K, Kaltschmitt M. Cost minimized hydrogen from solar and wind – Production and supply in the European catchment area. Energ Conver Manage 2022;265:115742. https://doi.org/10.1016/j.enconman.2022.115742.
[45] Towler GP, Sinnott RK. Chemical engineering design: Principles, practice, and economics of plant and process design. 2nd ed. Boston MA: Butterworth-Heinemann; 2013.
[46] Peters MS, Timmerhaus KD, West RE. Plant design and economics for chemical engineers. 5th ed. Boston: McGraw-Hill; 2006.
[47] Fasihi M, Breyer C. Baseload electricity and hydrogen supply based on hybrid PV-wind power plants. J Clean Prod 2020;243:118466. https://doi.org/10.1016/j.jclepro.2019.118466.
[48] Rodin V, Lindorfer J, Böhm H, Vieira L. Assessing the potential of carbon dioxide valorisation in Europe with focus on biogenic CO2. J CO2 Util 2020;41:101219. https://doi.org/10.1016/j.jcou.2020.101219.
[49] Young J, McQueen N, Charalambous C, Foteinis S, Hawrot O, Ojeda M, et al. The cost of direct air capture and storage can be reduced via strategic deployment but is unlikely to fall below stated cost targets. One Earth 2023;6(7):899–917. https://doi.org/10.1016/j.oneear.2023.06.004.
[50] Sievert K, Schmidt TS, Steffen B. Considering technology characteristics to project future costs of direct air capture. Joule 2024;8(4):979–99. https://doi.org/10.1016/j.joule.2024.02.005.
[51] Bundesministerium der Finanzen. AfA-Tabelle für den Wirtschaftszweig „Chemische Industrie“: § 193ff AO § 7 Abs 1 EStG; 1995.
[52] PTX Business Opportunity Analyser 2024.
[53] Smith E, Morris J, Kheshgi H, Teletzke G, Herzog H, Paltsev S. The cost of CO2 transport and storage in global integrated assessment modeling. Int J Greenhouse Gas Control 2021;109:103367. https://doi.org/10.1016/j.ijggc.2021.103367.
[54] Eurostat. Electricity prices for non-household consumers - bi-annual data (from 2007 onwards): Online data code: nrg_pc_205; Available from: https://ec.europa.eu/eurostat/databrowser/view/nrg_pc_205/default/table?lang=en.
[55] EZB. Jährliche Entwicklung des Wechselkurses des Euro gegenüber dem US-Dollar von 1999 bis 2022. [January 12, 2023]; Available from: https://de.statista.com/statistik/daten/studie/200194/umfrage/wechselkurs-des-euro-gegenueber-dem-us-dollar-seit-2001/.
[56] Kaiser P, Unde RB, Kern C, Jess A. Production of Liquid Hydrocarbons with CO 2 as Carbon Source based on Reverse Water-Gas Shift and Fischer-Tropsch Synthesis. Chem Ing Tech 2013;85(4):489–99. https://doi.org/10.1002/cite.201200179.
[57] Maitlis PM, de Klerk A. Greener Fischer-Tropsch Processes for Fuels and Feedstocks. Wiley; 2013.
[58] Rafati M, Wang L, Dayton DC, Schimmel K, Kabadi V, Shahbazi A. Techno-economic analysis of production of Fischer-Tropsch liquids via biomass gasification: The effects of Fischer-Tropsch catalysts and natural gas co-feeding. Energ Conver Manage 2017;133:153–66. https://doi.org/10.1016/j.enconman.2016.11.051.
[59] Panzone C, Philippe R, Chappaz A, Fongarland P, Bengaouer A. Power-to-Liquid catalytic CO2 valorization into fuels and chemicals: focus on the Fischer-Tropsch route. J CO2 Util 2020;38:314–47. https://doi.org/10.1016/j.jcou.2020.02.009.
[60] Ruokonen J, Nieminen H, Dahiru AR, Laari A, Koiranen T, Laaksonen P, et al. Modelling and Cost Estimation for Conversion of Green Methanol to Renewable Liquid Transport Fuels via Olefin Oligomerisation. Processes 2021;9(6):1046. https://doi.org/10.3390/pr9061046.